

Self-doping and the Mott-Kondo scenario for infinite-layer nickelate superconductors

Yi-feng Yang^{1,2,3,*} and Guang-Ming Zhang^{4,5,†}

¹*Beijing National Laboratory for Condensed Matter Physics and Institute of Physics,
Chinese Academy of Sciences, Beijing 100190, China*

²*School of Physical Sciences, University of Chinese Academy of Sciences, Beijing 100190, China*

³*Songshan Lake Materials Laboratory, Dongguan, Guangdong 523808, China*

⁴*State Key Laboratory of Low-Dimensional Quantum Physics and
Department of Physics, Tsinghua University, Beijing 100084, China*

⁵*Frontier Science Center for Quantum Information, Beijing 100084, China*

(Dated: December 27, 2021)

We give a brief review of the Mott-Kondo scenario and its consequence in the recently-discovered infinite-layer nickelate superconductors. We argue that the parent state is a self-doped Mott insulator and propose an effective t - J - K model to account for its low-energy properties. At small doping, the model describes a low carrier density Kondo system with incoherent Kondo scattering at finite temperatures, in good agreement with experimental observation of the logarithmic temperature dependence of electric resistivity. Upon increasing Sr doping, the model predicts a breakdown of the Kondo effect, which provides a potential explanation of the non-Fermi liquid behavior of the electric resistivity with a power law scaling over a wide range of the temperature. Unconventional superconductivity is shown to undergo a transition from nodeless ($d+is$)-wave to nodal d -wave near the critical doping due to competition of the Kondo and Heisenberg superexchange interactions. The presence of different pairing symmetry may be supported by recent tunneling measurements.

I. INTRODUCTION

Recent discovery of superconductivity (SC) in infinite-layer Sr-doped NdNiO₂ films¹ and subsequently in hole doped LaNiO₂ and PrNiO₂ films^{2–5} has stimulated intensive interest in condensed matter community. Despite of many theoretical and experimental efforts, there are still debates on its electronic structures and pairing mechanism^{6–13}. The study of possible Ni-based superconductivity was initially stimulated by cuprates, whose high T_c mechanism remains one of the most challenging topics in past three decades^{14–17}. Many attempts have been devoted to exploring new families of high T_c superconductors. Nickelate superconductors are but one latest example of these efforts.

In undoped cuprates, Cu²⁺ ions contain 9 electrons with partially occupied $3d_{x^2-y^2}$ orbitals. The oxygen $2p$ orbitals are higher in energy than the Cu $3d_{x^2-y^2}$ lower Hubbard band. Thus, cuprates belong to the so-called charge-transfer insulator. A superexchange interaction between localized Cu $3d_{x^2-y^2}$ spins is mediated by oxygen ions and causes an antiferromagnetic (AF) ground state. Upon chemical doping, holes may be introduced on the oxygen sites in the CuO₂ planes^{15–17} and combine with the $3d_{x^2-y^2}$ spins to form the Zhang-Rice singlets¹⁸, destroying the long-range AF order rapidly. In theory, these led to an effective t - J model, describing the holes moving on the antiferromagnetic square lattice. High temperature SC with robust d -wave pairing has been predicted and established over a wide doping range^{19–21}. Extending such “cuprate-Mott” conditions in other oxides has led to extensive efforts on nickel oxides^{22–32}. Nickelate superconductors have a similar layered crystal structure with Ni¹⁺ possessing the same $3d^9$ configuration as Cu²⁺. As a result, theories based on Mott scenario have

naturally been developed to account for nickelate superconductors.

However, there are clear evidences since the beginning suggesting that these two systems are different. Instead of a Mott insulator with AF long-range order like in cuprates, NdNiO₂ displays metallic behavior at high temperatures with a resistivity upturn below about 70 K, showing no sign of any magnetic long-range order in the whole measured temperature range³³. Similar results have previously been found in LaNiO₂ (Ref.³⁴). First-principles calculations have also revealed some subtle differences in their band structures. The O- $2p$ orbitals are located at a deeper energy compared to that of cuprates. Nd- $5d$ bands are found to hybridize with Ni- $3d$ bands and produce small electron pockets in the Brillouin zone. As a consequence, holes are doped directly into Ni- $3d$ orbitals rather than O- $2p$ orbitals. Nickelates should thus be modelled as a self-doped Mott insulator, which implies a multi-band system with two types of charge carriers, the itinerant Nd- $5d$ conduction electrons and the Ni- $3d_{x^2-y^2}$ holes, on a background lattice of Ni- $3d_{x^2-y^2}$ magnetic moments⁶. Joint analysis of the resistivity upturn and Hall coefficient at low temperatures suggests possible presence of incoherent Kondo scattering between low-density conduction electrons and localized Ni spins. A physical picture is illustrated in Fig. 1 on the square lattice. Then the basis for the Mott-Kondo scenario of nickelate superconductors has been established, leading to the proposal of an extended t - J - K model for a microscopic description of their low-energy properties^{6,7}.

Interestingly, the Kondo hybridization does not appear significant at first glance in band structure calculations²⁴. It was later realized that nickelates may host a special interstitial- s orbital for conduction electrons that have substantially stronger hybridization than previously

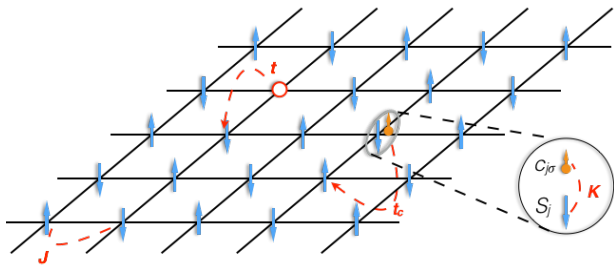


FIG. 1: Illustration of the effective model on a two-dimensional square lattice of NiO_2 plane of NdNiO_2 . Blue arrow represents Ni-spin, which interacts with its neighboring spin antiferromagnetically by coupling J . Orange arrow denotes Nd-5d electron, which couples to Ni-spin by the Kondo coupling K , to form a Kondo singlet (doublon). Red circle represents Ni- $3d^8$ configuration, or a holon. t_c and t denote the hopping of doublon and holon, respectively. Not shown is the holon-doublon annihilation into a Ni-spin. Figure adapted from Ref.⁶. Copyright 2020 by the American Physical Society.

thought³⁵. Resonant inelastic X-ray scattering (RIXS) measurements^{11,36} confirmed the presence of hybridization between Ni $3d_{x^2-y^2}$ and Nd $5d$ orbitals. At zero temperature, the self-doping effect and the Kondo coupling produce low-energy doublon (Kondo singlet) and holon excitations on the nickel spin-1/2 background. Because of the larger charge transfer energy, nickelates have a reduced superexchange interaction between Ni^{1+} spins by almost an order of magnitude than cuprates. Raman scattering measurements confirmed this expectation and estimated $J \approx 25 \text{ meV}$ in bulk NdNiO_2 ³⁷. The Kondo coupling may therefore suppress the AF long-range order and cause a phase transition to a paramagnetic metal⁶. The parent or underdoped compounds may therefore be viewed as a Kondo semimetal (KS). For large hole doping, the Ni- $3d$ electrons become more itinerant and the Kondo effect breaks down, followed by an abrupt change of the charge carriers. Indeed, a sign change of the Hall coefficient has been reported in experiment^{38,39}.

The above differences have an immediate impact on candidate pairing mechanism of the superconductivity. At critical doping, the t - J - K model predicted possible SC transition from a gapped ($d + is$)-wave state to a gapless d -wave pairing state due to the competition of Kondo and superexchange interactions⁷. Latest scanning tunneling experiment (STM) also revealed two different gap structures of U and V-shapes, supporting the possibility of above scenario. Thus, nickelates may belong to a novel class of unconventional superconductors and one may anticipate potentially more interesting properties bridging the cuprates and heavy fermions.

In this paper, we briefly summarize the consequences of the Mott-Kondo scenario based on the extended t - J - K model for nickelate superconductors^{6,7}. We propose a global phase diagram upon electron and hole doping and derive a low-energy effective Hamiltonian with doublon and holon excitations in the low doping region. We then

employ the renormalized mean-field theory (RMFT) to study the possibility of superconductivity and predict a phase transition of its pairing symmetry. The latter is shown to originate from the breakdown of Kondo hybridization, accompanied with non-Fermi liquid (NFL) behavior of the resistivity $\rho \sim T^\alpha$ near critical doping.

II. THEORY

A. Model Hamiltonian

To introduce the effective t - J - K model for describing the low-energy physics of nickelates, we start from a background lattice of Ni^{1+} $3d_{x^2-y^2}$ localized spins with a small number of self-doped holes and Nd- $5d$ conduction electrons⁶. Similar to cuprates, one expects an AF superexchange interaction between Ni^{1+} spins through the O- $2p$ orbitals. This is different from heavy fermion systems, where the exchange interaction between localized spins originates from the Ruderman-Kittel-Kasuya-Yosida (RKKY) interaction mediated by conduction electrons. The motion of holes on the spin lattice should be strongly renormalized as in the usual t - J model. There is an additional local Kondo interaction between local spins and conduction electrons. The total Hamiltonian therefore contains three terms:

$$H = H_t + H_J + H_K, \quad (1)$$

where the first term comes from the hopping of holes, the second term describes the spin lattice, and the third term gives the Kondo interaction.

For simplicity, we consider a minimal model with Ni- $3d^8$ and Nd- $5d^0$ as the vacuum. As in cuprates, the localized $3d_{x^2-y^2}$ spins on the NiO_2 plane can be described by a two-dimensional quantum Heisenberg model with nearest neighbour AF superexchange interactions,

$$H_J = J \sum_{\langle ij \rangle} S_i \cdot S_j, \quad (2)$$

whose ground state is a Mott insulator with AF long-range orders.

The self-doping effect is supported by first-principles band structure calculations⁴⁰, where the Nd $5d$ orbitals in NdNiO_2 are found to hybridize with the Ni $3d$ orbitals and give rise to small electron pockets in the Brillouin zone. Thus, we have a small number of Nd- $5d$ conduction electrons. This is actually supported by experiment. At high temperatures, the Hall coefficient is dominated by conduction electrons giving $R_H \approx -4 \times 10^{-3} \text{ cm}^3 \text{ C}^{-1}$ for NdNiO_2 and $-3 \times 10^{-3} \text{ cm}^3 \text{ C}^{-1}$ for LaNiO_2 . By contrast, in typical heavy fermion metals such as CeMIn_5 ($M = \text{Co, Rh, Ir}$), we have $R_H \approx -3.5 \times 10^{-4} \text{ cm}^3 \text{ C}^{-1}$ at high temperatures⁴¹. The larger and negative values of the Hall coefficient implies that there are only a few percent of electron-like carriers per unit cell in NdNiO_2 and LaNiO_2 .

The hybridization between Ni $3d_{x^2-y^2}$ spins and conduction electrons gives the additional Kondo term:

$$H_K = -t_c \sum_{\langle ij \rangle, \sigma} \left(c_{i\sigma}^\dagger c_{j\sigma} + h.c. \right) + \frac{K}{2} \sum_{j\alpha; \sigma\sigma'} S_j^\alpha c_{j\sigma}^\dagger \tau_{\sigma\sigma'}^\alpha c_{j\sigma'}, \quad (3)$$

where $\epsilon_{\mathbf{k}}$ is the dispersion of conduction electrons projected on the square lattice of the Ni¹⁺ ions, and τ^α ($\alpha = x, y, z$) are the spin-1/2 Pauli matrices. Only a single conduction band is considered for simplicity. In reality, the pockets should be three dimensional. For a low carrier density system, the average number of conduction electrons is small, i.e. $n_c = N_s^{-1} \sum_{j\sigma} \langle c_{j\sigma}^\dagger c_{j\sigma} \rangle \ll 1$.

The presence of magnetic impurities may be at first glance ascribed to the Nd 4*f* moments. However, the Nd³⁺ ion contains three *f* electrons forming a localized spin-3/2 moment, which acts more like a classical spin as in manganites and therefore disfavors spin-flip scattering as the quantum spin-1/2 moment. Their energy level is also far away from the Fermi energy, so it is reasonable to ignore the Nd 4*f* electrons.

For parent compounds, self-doping also introduces an equal number of Ni $3d_{x^2-y^2}$ holes on the spin lattice. The hopping of holes on the lattice of Ni $3d_{x^2-y^2}$ spins can be described as interactions,

$$H_t = - \sum_{ij\sigma} \left(t_{ij} P_G d_{i\sigma}^\dagger d_{j\sigma} P_G + h.c. \right), \quad (4)$$

where $d_{i\sigma}$ and $d_{i\sigma}^\dagger$ are the annihilation and creation operators of the Ni $3d_{x^2-y^2}$ electrons, respectively, t_{ij} is the hopping integral between site *i* and *j*, and P_G is the Gutzwiller operator to project out doubly occupancy of local Ni $3d_{x^2-y^2}$ orbital. As in cuprates, the holes' motion is strongly renormalized due to the onsite Coulomb repulsion *U*.

Quite generally, the effective *t-J-K* model can be replaced by the one-band Hubbard model plus a hybridization term with additional conduction electrons:

$$H = \sum_{\mathbf{k}\sigma} E_{\mathbf{k}} d_{\mathbf{k}\sigma}^\dagger d_{\mathbf{k}\sigma} + U \sum_i n_{i\uparrow}^d n_{i\downarrow}^d + \sum_{\mathbf{k}\sigma} \epsilon_{\mathbf{k}} c_{\mathbf{k}\sigma}^\dagger c_{\mathbf{k}\sigma} + \sum_{\mathbf{k}\sigma} V_{\mathbf{k}} \left(d_{\mathbf{k}\sigma}^\dagger c_{\mathbf{k}\sigma} + h.c. \right). \quad (5)$$

The model may also be viewed as a periodic Anderson model with dispersive *d* bands. It allows for a better treatment of charge fluctuations of the Ni $3d_{x^2-y^2}$ orbitals, in particular for large Sr doping or small Coulomb interaction. In this work, we only consider the minimal *t-J-K* model and show that it can already capture some main physics of the nickelates.

B. Global phase diagram

As is in heavy fermion systems, the *t-J-K* model contains two competing energy scales that support different

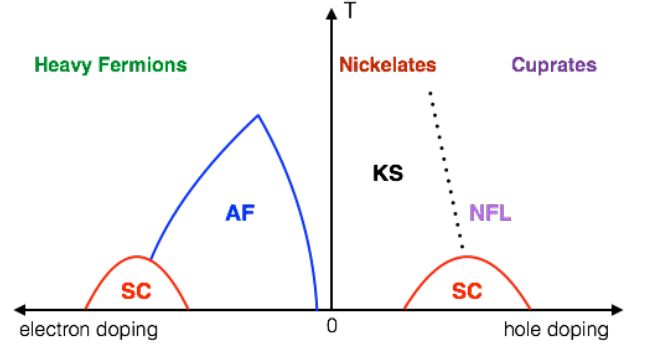


FIG. 2: A schematic phase diagram of the *t-J-K* model with electron and hole doping. KS stands for incoherent Kondo scattering or Kondo semimetal. Whether or not the AF phase may exist depends on details of electron and hole densities introduced by doping.

ground states. The Heisenberg superexchange *J* favors an antiferromagnetic long-range order, while the Kondo coupling *K* tends to screen the local spins and form a nonmagnetic ground state. In nickelates, due to the large charge transfer energy between O-2*p* and Ni-3*d*_{*x*²-*y*²} orbitals, *J* is expected to be smaller than that (about 100 meV) in cuprates. Raman scattering measurements confirmed this expectation and estimated $J \approx 25$ meV in bulk NdNiO₂³⁷. First-principles calculations also suggested *J* of the order of 10 meV³⁵. There is at present no direct measurement of the Kondo interaction *K*. However, from the observed resistivity minimum at 70-100 K in NdNiO₂ and LaNiO₂^{1,34}, *K* may be roughly estimated to be of the order of a few hundred meV^{6,35,42}. Thus for undoped nickelates, the Kondo coupling is a relatively large energy scale.

We may propose a global phase diagram starting from an antiferromagnetic ground state. The self-doping introduces equal numbers of conduction electrons and holes. The conduction electrons tend to form Kondo singlets with local spins due to the large *K*. Both tend to suppress the long-range AF order and causes a paramagnetic ground state. But because of the small number of conduction electrons, local spins cannot be fully Kondo screened to become delocalized. Thus, instead of a heavy fermion metal, we are actually dealing with a low carrier density Kondo system at low temperatures. Due to insufficient Kondo screening, the resistivity exhibits insulating-like behavior (upturn) because of incoherent Kondo scattering, which is typical for low carrier density Kondo systems and has been observed previously in CeNi_{2- δ} (As_{1-*x*}P_{*x*})₂⁴³ and NaYbSe₂⁴⁴.

Upon Sr (hole) doping, the number of conduction electrons may be reduced, while that of holes increases. The Kondo physics may be suppressed and replaced by the usual *t-J* model for large hole doping, resembling the physics of cuprates. On the other hand, for electron doping, we may expect to first recover the AF long-range order with reduced hole density, and then with increas-

ing conduction electrons and Kondo screening, the AF order will be suppressed again and the system turns into a heavy fermion metal with sufficient electron doping. SC may emerge around the quantum critical point. Whether or not the AF phase may actually exist depends on how doping changes the fraction of electron and hole carriers. But in bulk $\text{Nd}_{1-x}\text{Sr}_x\text{NiO}_2$, NMR experiment has revealed short-range glassy AF ordering, supporting the possible existence of antiferromagnetism⁴⁵. Figure 2 summarizes possible ground states of the model on the temperature-doping plane, showing a connection between the heavy fermion and cuprate physics on two ends and the nickelates in between. However, it should be noted that current experiment on “overdoped” nickelate superconductors found a weak insulator rather than a Fermi liquid as in heavily hole-doped cuprates³⁹. How exactly holes are doped in $\text{Nd}_{1-x}\text{Sr}_x\text{NiO}_2$ remains an open question.

C. Low energy excitations

As shown in the phase diagram, the paramagnetic region (KS) is responsible for undoped or low doped nickelates. In this case, we have a small number (n_c) of conduction electrons per Ni-site and $n_c + p$ empty nickel sites (holons) on the NiO_2 plane, where p is the hole doping ratio. In the large K limit and at zero temperature, conduction electrons form Kondo singlets or doublons with local Ni spins. We may then derive an effective low-energy Hamiltonian in terms of doublons, holons, and localized spins, to describe a doped Mott metallic state with Kondo singlets. A cartoon picture is given in Fig. 1.

For this, we first introduce the pseudofermion representation for the spin-1/2 local moments:

$$S_j^+ = f_{j\uparrow}^\dagger f_{j\downarrow}, S_j^- = f_{j\downarrow}^\dagger f_{j\uparrow}, S_j^z = \frac{1}{2} (f_{j\uparrow}^\dagger f_{j\uparrow} - f_{j\downarrow}^\dagger f_{j\downarrow}),$$

where $f_{j\sigma}$ is a fermionic operator for the spinon on site j . The Ni $3d_{x^2-y^2}$ electron operator is given by $d_{j\sigma} = h_j^\dagger f_{j\sigma}$ with a local constraint, $h_j^\dagger h_j + \sum_\sigma f_{j\sigma}^\dagger f_{j\sigma} = 1$, if we ignore double occupancy. Here h_j^\dagger is a bosonic operator creating a holon on site j .

The doublon operators for the on-site Kondo spin singlet and triplets may be defined as

$$b_{j0}^\dagger = \frac{1}{\sqrt{2}} (f_{j\uparrow}^\dagger c_{j\downarrow}^\dagger - f_{j\downarrow}^\dagger c_{j\uparrow}^\dagger);$$

$$b_{j1}^\dagger = f_{j\uparrow}^\dagger c_{j\uparrow}^\dagger, b_{j2}^\dagger = \frac{1}{\sqrt{2}} (f_{j\uparrow}^\dagger c_{j\downarrow}^\dagger + f_{j\downarrow}^\dagger c_{j\uparrow}^\dagger), b_{j3}^\dagger = f_{j\downarrow}^\dagger c_{j\downarrow}^\dagger.$$

The Kondo term then becomes

$$\frac{K}{2} \sum_{j\alpha;\sigma\sigma'} S_j^\alpha c_{j\sigma}^\dagger \tau_{\sigma\sigma'}^\alpha c_{j\sigma'} = \frac{K}{4} \sum_{\mu=1}^3 b_{j\mu}^\dagger b_{j\mu} - \frac{3K}{4} \sum_j b_{j0}^\dagger b_{j0}, \quad (6)$$

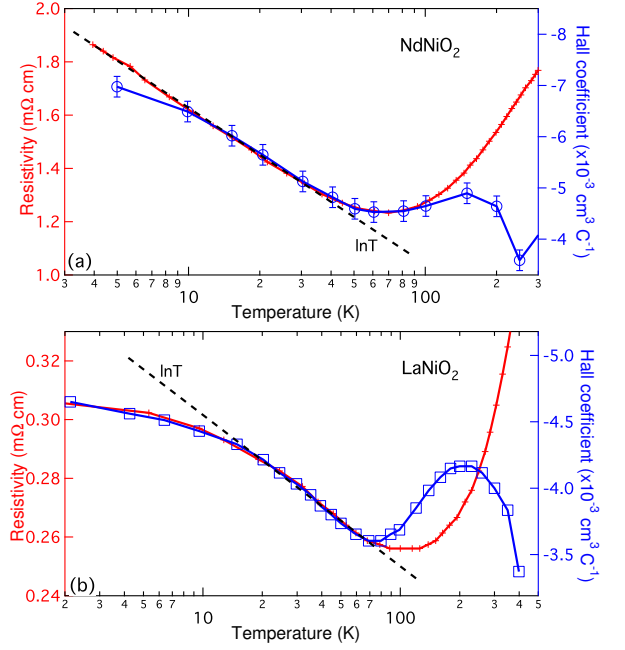


FIG. 3: Logarithmic temperature dependence of the resistivity (red color) and the Hall coefficient (blue color) at low temperatures for (a) NdNiO_2 with the experimental data adopted from Ref.¹; (b) LaNiO_2 reproduced from Ref.³⁴. The dashed lines are the $\ln T$ fits. Figure adapted from Ref.⁶. Copyright 2020 by the American Physical Society.

which describes the doublon formation on each site, namely, the Kondo singlet or triplet pair formed by one conduction electron with a localized spinon. We see that the triplet pair costs a higher energy of K . Similarly, there may also exist three-particle states with one localized spinon and two conduction electrons on the same site, $e_{j\sigma}^\dagger = f_{j\sigma}^\dagger c_{j\uparrow}^\dagger c_{j\downarrow}^\dagger$, or one-particle states with one unpaired spinon only, $\tilde{f}_{j\sigma} = (1 - n_j^c) f_{j\sigma}$.

Following Refs.^{46,47}, we first rewrite the Hamiltonian in terms of these new operators and then eliminate all high-energy terms containing $b_{j\mu}$ ($\mu = 1, 2, 3$) and $e_{j\sigma}$ using canonical transformation while keeping only the on-site doublon (b_{j0}) and unpaired spinons ($\tilde{f}_{j\sigma}$). This yields an effective low-energy model with a simple form

$$H_{\text{eff}} = -t \sum_{\langle ij \rangle, \sigma} (h_i \tilde{f}_{i\sigma}^\dagger \tilde{f}_{j\sigma} h_j^\dagger + h.c.) + J \sum_{\langle ij \rangle} \tilde{S}_i \cdot \tilde{S}_j - \frac{t_c}{2} \sum_{\langle ij \rangle, \sigma} (b_{i0}^\dagger \tilde{f}_{i\sigma} \tilde{f}_{j\sigma}^\dagger b_{j0} + h.c.), \quad (7)$$

where the spin operators are $\tilde{S}_j^\alpha = \sum_{\sigma\sigma'} \tilde{f}_{j\sigma}^\dagger \frac{1}{2} \tau_{\sigma\sigma'}^\alpha \tilde{f}_{j\sigma'}$ with a local constraint $h_j^\dagger h_j + b_{j0}^\dagger b_{j0} + \sum_\sigma \tilde{f}_{j\sigma}^\dagger \tilde{f}_{j\sigma} = 1$. Here only the nearest-neighbor hopping parameters t and t_c are considered for simplicity. For large but finite K , apart from some complicated interactions, an additional

term should also be included

$$H_b = -\frac{3}{4} \left(K + \frac{t_c^2}{K} \right) \sum_j b_{j0}^\dagger b_{j0} + \frac{5t_c^2}{12K} \sum_{\langle ij \rangle} b_{i0}^\dagger b_{i0} b_{j0}^\dagger b_{j0}, \quad (8)$$

which describes the doublon condensation.

This effective Hamiltonian describes the ground state of nickelates at zero or low doping. It is similar to the usual t - J model for cuprates¹⁸, but includes two types of mobile quasiparticles: doublons (Kondo singlets) and holons. It is now clear why the self-doping can efficiently suppress the AF long-range order to yield a paramagnetic ground state in nickelates. At high temperatures, doublons become deconfined, causing incoherent Kondo scattering in transport measurements. This is confirmed by the resistivity replotted in Fig. 3 as a function of temperature for both NdNiO₂ and LaNiO₂. Unlike cuprates, the resistivity exhibits metallic behavior at high temperature but shows an upturn below about 70 K. If we put the data on a linear-log scale, we find that the upturn follows exactly a logarithmic temperature ($\ln T$) dependence over a large temperature range for both compounds, which is a clear evidence for incoherent Kondo scattering typical for low carrier density Kondo systems⁴⁸. The saturation at very low temperatures is an indication of Kondo screening. This Kondo scenario is also supported by the Hall measurement. In both compounds, the Hall coefficient R_H exhibits non-monotonic temperature dependence. It approaches a negative constant at high temperatures due to the contribution of conduction electrons, but exhibits the same $\ln T$ dependence at low temperatures. The linear relation $R_H \propto \rho$ is an indication of skew scattering by localized magnetic impurities in typical Kondo systems^{49,50}.

An alternative explanation for the resistivity upturn is weak localization, where disordered holes in the NiO₂ plane may also give rise to a logarithmic correction. However, this explanation is not supported by the corresponding correction to the Hall coefficient and magnetoresistance.

D. Superconductivity

Experimentally, superconductivity was first observed to emerge and have an onset temperature of 14.9 K in 20% Sr doped NdNiO₂ thin films deposited on SrTiO₃ substrates¹. From the t - J - K model, one may naively expect that sufficiently large doping may deplete conduction electrons and increase the number of holons, driving the system to an effective t - J model resembling that in cuprates. As a result, d -wave superconductivity may arise due to the superexchange interaction between Ni $3d_{x^2-y^2}$ electrons. However, this is not the whole truth. With increasing Sr doping, the ordinary Hall coefficient at high temperatures becomes smaller in magnitude but remains negative even in Nd_{0.8}Sr_{0.2}NiO₂¹, which cannot be explained by a single carrier model but rather indi-

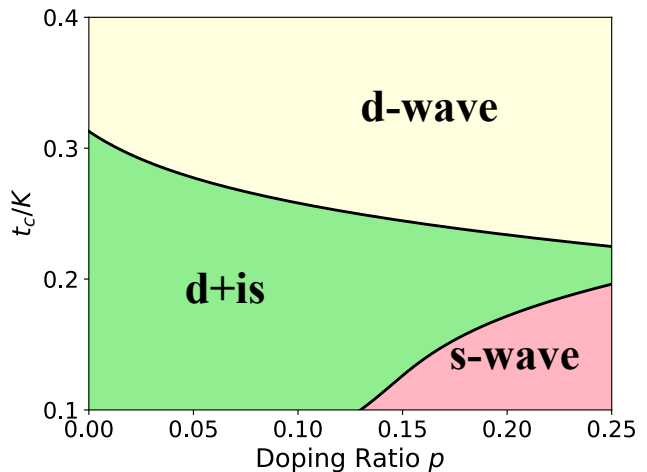


FIG. 4: Phase diagram of the superconductivity. At small hole concentration p , the pairing symmetry is primarily ($d + is$)-wave SC. At large doping p , the pairing is either s -wave SC for small hopping t_c/K or d -wave SC for large hopping t_c/K . Figure adapted from Ref.⁷. Copyright 2020 by the American Physical Society.

cates a cancellation of electron and hole contributions. Thus, conduction electrons should still be present even at 20% Sr doping. It is thus anticipated that superconductivity in nickelates may be affected by the presence of conduction electrons and their Kondo hybridization with Ni $3d_{x^2-y^2}$ electrons.

The pairing symmetry can be studied by using the renormalized mean-field theory (RMFT)^{7,51}, which had successfully predicted the d -wave superconductivity in the t - J model for cuprates and can well describe the Fermi liquid similar to the slave-boson mean field theory. Our numerical calculations of superconductivity on the generalized t - J - K model have yielded a typical superconducting phase diagram in Fig. 4. The pairing symmetry is found to depend on the hole concentration p and the effective strength of the Kondo hybridization controlled by the conduction electron hopping (t_c/K) ⁶. For simplicity, we have taken the Kondo coupling K as the energy unit ($K = 1$), and set the AF Heisenberg spin exchange $J = 0.1$. Both the nearest-neighbor hopping $t = 0.2$ and the next-nearest-neighbor hopping $t' = -0.05$ are taken into consideration for Ni $3d$ electrons. The density of conduction electrons is taken to be $n_c = 0.1$, while their nearest-neighbor hopping t_c is chosen as a tuning parameter.

For all doping, we find a dominant d -wave pairing symmetry for large t_c/K or small K . But for low doping and moderate t_c/K , we obtain a ($d + is$)-wave pairing state that breaks the time-reversal symmetry. This is different from the conventional picture based purely on the t - J model for cuprates, where the Heisenberg superexchange interaction favors d -wave pairing⁵². The s -wave pairing should be ascribed to the Kondo coupling, which is an on-site spin exchange between localized and conduction

electrons⁵³. This is supported by the extended s -wave solution at large doping for small t_c/K or strong Kondo coupling. It is the combination of both effects that gives rise to the special $(d + is)$ -wave superconductivity and represents a genuine feature of the nickelate superconductivity differing from cuprates or heavy fermions.

Details of RMFT calculations are explained as follows⁷. We first introduce three Gutzwiller renormalization factor to approximate the operator that projects out the doubly occupied states: $g_t = n_h/(1 + n_h)$ for the hopping t and t' , $g_J = 4/(1 + n_h)^2$ for the superexchange J , and $g_K = 2/(1 + n_h)$ for the Kondo coupling K . We then define four mean-field order parameters to decouple the Heisenberg superexchange and Kondo terms:

$$\begin{aligned}\chi_{ij} &= \langle d_{i\uparrow}^\dagger d_{j\uparrow} + d_{i\downarrow}^\dagger d_{j\downarrow} \rangle, & B &= \frac{1}{\sqrt{2}} \langle d_{j\uparrow}^\dagger c_{j\downarrow}^\dagger - d_{j\downarrow}^\dagger c_{j\uparrow}^\dagger \rangle, \\ \Delta_{ij} &= \langle d_{i\uparrow}^\dagger d_{j\downarrow}^\dagger - d_{i\downarrow}^\dagger d_{j\uparrow}^\dagger \rangle, & D &= \frac{1}{\sqrt{2}} \langle c_{j\uparrow}^\dagger d_{j\uparrow} + c_{j\downarrow}^\dagger d_{j\downarrow} \rangle.\end{aligned}$$

The resulting mean-field Hamiltonian has a simple bilinear form in the momentum space,

$$\mathcal{H}_{\text{mf}} = \sum_{\mathbf{k}} \Psi_{\mathbf{k}}^\dagger \begin{pmatrix} \chi(\mathbf{k}) & K_D & \Delta^*(\mathbf{k}) & K_B^* \\ K_D^* & \epsilon(\mathbf{k}) & K_B^* & 0 \\ \Delta(-\mathbf{k}) & K_B & -\chi(-\mathbf{k}) & -K_D^* \\ K_B & 0 & -K_D & -\epsilon(-\mathbf{k}) \end{pmatrix} \Psi_{\mathbf{k}}, \quad (9)$$

where we have introduced the Nambu spinors $\Psi_{\mathbf{k}}^\dagger = (d_{\mathbf{k}\uparrow}^\dagger, c_{\mathbf{k}\uparrow}^\dagger, d_{-\mathbf{k}\downarrow}, c_{-\mathbf{k}\downarrow})$ and defined the matrix elements

$$\begin{aligned}\chi(\mathbf{k}) &= -\sum_{\alpha} \left(t g_t + \frac{3}{8} J g_J \chi_{\alpha} \right) \cos(\mathbf{k} \cdot \alpha) \\ &\quad - t' g_t \sum_{\delta} \cos(\mathbf{k} \cdot \delta) + \mu_1, \\ \epsilon(\mathbf{k}) &= -t_c \sum_{\alpha} \cos(\mathbf{k} \cdot \alpha) + \mu_2, \\ \Delta(\mathbf{k}) &= -\frac{3}{8} J g_J \sum_{\alpha} \Delta_{\alpha} \cos(\mathbf{k} \cdot \alpha), \\ K_D &= -\frac{3}{4} g_K K \frac{D}{\sqrt{2}}, K_B = -\frac{3}{4} g_K K \frac{B}{\sqrt{2}}.\end{aligned} \quad (10)$$

Here α denotes the vectors of the nearest-neighbor lattice sites and δ stands for those of the next-nearest-neighbor sites. μ_1 and μ_2 are chemical potentials fixing the numbers of the constrained electrons $d_{i\sigma}$ and conduction electrons $c_{i\sigma}$, respectively.

The above mean-field Hamiltonian can be diagonalized using the Bogoliubov transformation, $(d_{\mathbf{k}\uparrow}, c_{\mathbf{k}\uparrow}, d_{-\mathbf{k}\downarrow}^\dagger, c_{-\mathbf{k}\downarrow}^\dagger)^T = U_{\mathbf{k}} (\alpha_{\mathbf{k}\uparrow}, \beta_{\mathbf{k}\uparrow}, \alpha_{-\mathbf{k}\downarrow}^\dagger, \beta_{-\mathbf{k}\downarrow}^\dagger)^T$. The ground state is given by the vacuum of the Bogoliubov quasiparticles $\{\alpha_{\mathbf{k}\sigma}, \beta_{\mathbf{k}\sigma}\}$, which in turn yields the self-consistent equations for the mean-field order parameters. We will not go into more details here, but only mention that the mean-field self-consistent equations can be solved numerically and yield two dominant pairing

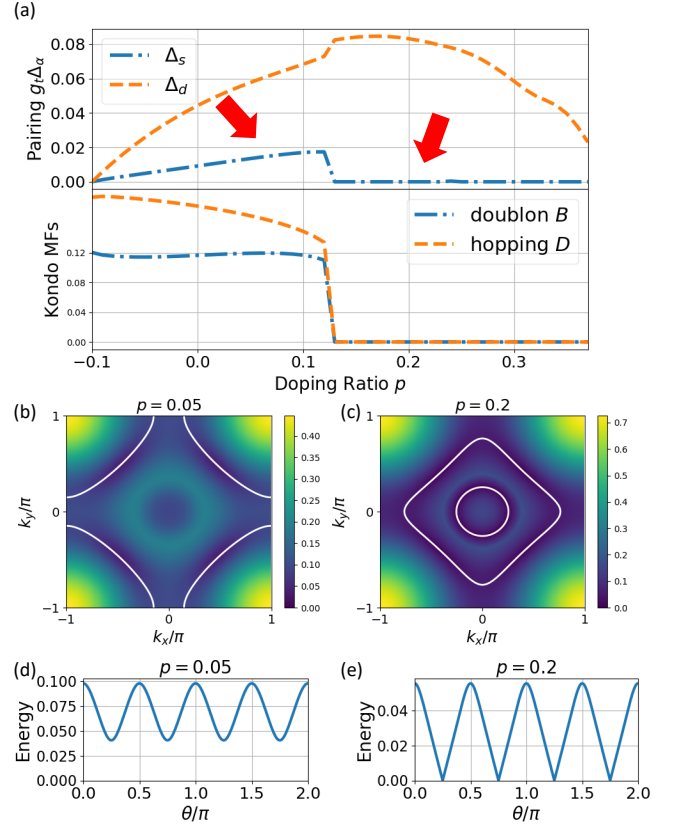


FIG. 5: RMFT results for $t_c/K = 0.25$. (a) The mean-field parameters as a function of doping for $g_t \Delta$ (upper panel) and B and D (lower panel). (b) and (c) show the quasiparticle excitation energy (background) and the Fermi surface (white solid line) defined as the minimal excitation energy at $p = 0.05$ ($d + is$)-wave and $p = 0.2$ (d -wave) as marked by the arrows in (a). (d) and (e) displayed the respective superconducting gap along the Fermi surface. Figure adapted from Ref.⁷. Copyright 2020 by the American Physical Society.

channels of s and d -waves as shown in the phase diagram Fig. 4. Typical results for the mean-field parameters are plotted in Fig. 5(a) as a function of the doping ratio p for $t_c/K = 0.25$. For clarity, we have defined $\Delta_s = |\Delta_x + \Delta_y|/2$ and $\Delta_d = |\Delta_x - \Delta_y|/2$ to represent the respective pairing amplitudes of s and d channels. We see a clear transition from the mixed $(d + is)$ -wave SC to the pure d -wave SC.

Antiferromagnetic spin fluctuations have been observed in bulk $\text{Nd}_{1-x}\text{Sr}_x\text{NiO}_2$ by NMR⁴⁵ and may also exist and play the role of pairing glues in thin films. Hence the presence of a dominant d -wave pairing at large doping is expected from the experience in cuprates. However, our results also suggest several additional features of the nickelate superconductivity that are not present in cuprates and may be examined in experiment. First, for sufficiently large Kondo coupling K , the $(d + is)$ -wave SC in the low doping region breaks the time reversal symmetry and as shown in Fig. 5(d), has a nodeless gap

which is distinctly different from the usual d -wave pairing with nodes along the diagonal direction. Second, we predict a quantum phase transition between this gapped ($d + is$)-wave SC to the nodal d -wave superconductivity with increasing hole doping. These features can be detected by scanning tunneling, penetration depth, or μ SR experiment and serve as a support for our theory. We remark that conduction electrons play an important role in our theory of nickelate superconductivity, which is not possible in the single-band Mott picture. The importance of electron pockets is in fact supported by experimental measurements of the upper critical field^{54,55}.

Recent single particle tunneling experiment⁵⁶ on superconducting nickelate thin films have also observed two distinct types of spectra: a V-shape feature with a gap maximum of 3.9 meV, a U-shape feature with a gap of about 2.35 meV, and some spectra with mixed contributions of these two components. If we attribute their different observations to different hole concentrations due to possible surface effect, the two types of spectra may correspond exactly to the two pairing states in our theory. In this sense, the scanning tunneling spectra have provided a supportive evidence for our theoretical prediction of multiple superconducting phases. Of course, the ($d + is$)-wave pairing might not exist in real materials if the Kondo coupling K is too weak or t_c/K is too large. In that case, as is seen in Fig. 4, d -wave pairing may become dominant on the hole Fermi surface, but electron pockets may still have nodeless gap depending on their position in the Brillouin zone.

E. Quantum criticality

As shown in Fig. 5, for moderate t_c/K , the SC transition from ($d + is$) to d -wave is accompanied with vanishing Kondo mean-field parameters B and D , which implies a breakdown of the Kondo hybridization in the large doping side. Correspondingly, the Fermi surface structures also change from a large hole-like Fermi surface around four Brillouin zone corners at low doping to two separate electron-like Fermi surfaces (from decoupled charge carriers) around the Brillouin zone center at large doping. These results may be compared with the Hall experiments in $\text{Nd}_{1-x}\text{Sr}_x\text{NiO}_2$ ^{38,39}, which revealed a crossover line of sign change in the temperature-doping phase diagram near the maximal T_c . The line marks a potential change in the Fermi surfaces and resembles that observed in some heavy fermion systems owing to the delocalization of localized moments⁵⁷. It is thus attempted to link the experiment with our theoretical proposals and predict a zero-temperature quantum critical point with the SC transition and the Fermi surface change near the crossover line, although it should be cautious that they take place in different temperature region.

As a matter of fact, experiment has indeed observed quantum critical behavior in the normal state above T_c . A tentative fit of the resistivity in superconducting nick-

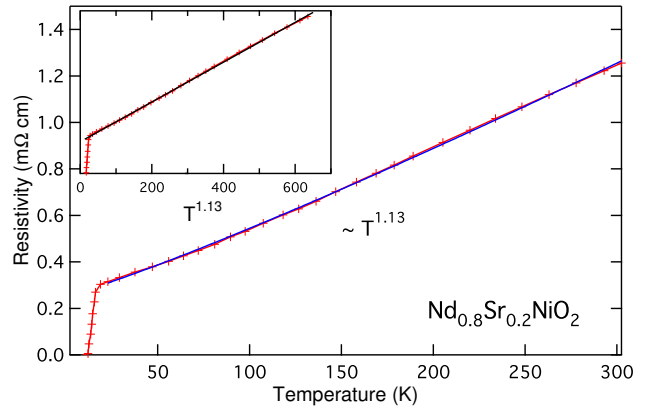


FIG. 6: Power-law temperature dependence of the electric resistivity above $T_c = 15$ K up to the room temperature for $\text{Nd}_{0.8}\text{Sr}_{0.2}\text{NiO}_2$. The experimental data were reproduced from Ref.¹.

elate thin films has yielded power-law scaling with temperature, namely $\rho \sim T^\alpha$, with $\alpha = 1.1 - 1.3$ over a wide range⁶. Figure 6 gives an example of the fit in $\text{Nd}_{0.8}\text{Sr}_{0.2}\text{NiO}_2$ and we obtain $\alpha \approx 1.13$ from slightly above T_c up to the room temperature. This reminds us the strange metal above T_c in optimal-doped cuprates and the non-Fermi liquid in heavy fermion systems. Better numerical calculations are required in order to establish the exact mechanism of this scaling.

III. FUTURE PERSPECTIVE

We have introduced the picture of self-doped Mott insulator to describe the recently discovered nickelate superconductors. The self-doping effect has been generally accepted by the community and distinguishes nickelates from cuprates. We further propose a Mott-Kondo scenario and an extended t - J - K model based on transport measurements and electronic structure calculations. Our model bridges the usual Kondo lattice model for heavy fermions and the t - J model for cuprates, but shows unique features that can only be understood as an interplay of both physics. Our theory provides a natural explanation of the resistivity upturn in undoped nickelates at low temperatures, and our calculations based on the t - J - K model predict an exotic ($d + is$)-wave superconductivity that breaks the time reversal symmetry and a possible transition of the pairing symmetry at critical doping, around which the normal state exhibits non-Fermi liquid behavior above T_c . This implies that nickelate superconductors are a novel class of unconventional superconductors. Thus, exploration of new physics based on our theory will be an interesting direction for future investigations.

Currently there still exist different opinions on the effect of Sr doping. Some argued that holes may occupy

other Ni $3d$ orbitals and the Hund coupling may favor a high spin state ($S = 1$). This scenario seems inconsistent with joint analyses of XAS and RIXS experiments⁵⁸ and a number of other calculations⁹. Nevertheless, our model allows for a straightforward multi-orbital extension by considering a two-band Hubbard model of Ni $3d$ orbitals (or its projection at large U) plus hybridization with additional conduction bands. So far, bulk nickelates have not been found superconductive and many issues remain to be answered both in theory and in experiment⁵⁹. Our proposal of the self-doping effect, the Mott-Kondo scenario, and the t - J - K model provides a promising starting

basis for future investigations.

IV. ACKNOWLEDGMENTS

This work was supported by the National Natural Science Foundation of China (11774401, 11974397, 12174429), the National Key Research and Development Program of MOST of China (2017YFA0303103, 2017YFA0302902), and the Strategic Priority Research Program of CAS (Grand No. XDB33010100).

-
- * yifeng@iphy.ac.cn
† gmzhang@tsinghua.edu.cn
- ¹ D. Li *et al.*, Nature **572**, 624 (2019).
 - ² M. Osada *et al.*, Nano Lett. **20**, 5735 (2020).
 - ³ M. Osada *et al.*, Phys. Rev. Materials **4**, 121801(R) (2020).
 - ⁴ S. W. Zeng *et al.*, arXiv:2105.13492.
 - ⁵ M. Osada *et al.*, arXiv:2105.13494.
 - ⁶ G.-M. Zhang, Y.-F. Yang, and F.-C. Zhang, Phys. Rev. B **101**, 020501(R) (2020).
 - ⁷ Z. Wang, G.-M. Zhang, Y.-F. Yang, and F.-C. Zhang, Phys. Rev. B **102**, 220501(R) (2020).
 - ⁸ A. S. Botana and M. R. Norman, Phys. Rev. X **10**, 011024 (2020).
 - ⁹ M. Jiang, M. Berciu, and G. Sawatzky, Phys. Rev. Lett. **124**, 207004 (2020).
 - ¹⁰ H. Sakakibara *et al.*, Phys. Rev. Lett. **125**, 077003 (2020).
 - ¹¹ M. Hepting *et al.*, Nat. Mater. **19**, 381 (2020).
 - ¹² Y. Normura *et al.*, arXiv:1909.03942 (2019).
 - ¹³ J. Gao, Z. Wang, C. Fang, and H. Weng, Natl. Sci. Rev. **8**, nwaa218 (2021).
 - ¹⁴ J. P. Bednorz and K. A. Muller, Z. Phys. B **64**, 189 (1986).
 - ¹⁵ P. W. Anderson, Science **235**, 1196 (1987).
 - ¹⁶ P. W. Anderson *et al.*, J. Phys.: Condens. Matter **16**, R755 (2004).
 - ¹⁷ P. A. Lee, N. Nagaosa, and X. G. Wen, Rev. Mod. Phys. **78**, 17 (2006).
 - ¹⁸ F. C. Zhang and T. M. Rice, Phys. Rev. B **37**, 3759 (1988).
 - ¹⁹ Z. X. Shen *et al.*, Phys. Rev. Lett. **70**, 1553 (1993).
 - ²⁰ D. A. Wollman *et al.*, Phys. Rev. Lett. **71**, 2134 (1993).
 - ²¹ C. C. Tsuei *et al.*, Phys. Rev. Lett. **73**, 593 (1994).
 - ²² V. I. Anisimov, D. Bukhvalov, and T. M. Rice, Phys. Rev. B **59**, 7901-7906 (1999).
 - ²³ M. A. Hayward, M. A. Green, M. J. Rosseinsky, and J. Sloan, J. Am. Chem. Soc. **121**, 8843 (1999).
 - ²⁴ K.-W. Lee and W. E. Pickett, Phys. Rev. B **70**, 165109 (2004).
 - ²⁵ A. S. Botana, V. Pardo, and M. R. Norman, Phys. Rev. Materials **1**, 021801(R) (2017).
 - ²⁶ J. Chaloupka and G. Khaliullin, Phys. Rev. Lett. **100**, 016404 (2008).
 - ²⁷ P. Hansmann *et al.*, Phys. Rev. Lett. **103**, 016401 (2009).
 - ²⁸ S. Middey *et al.*, Annu. Rev. Mater. Res. **46**, 305 (2016).
 - ²⁹ A. V. Boris *et al.*, Science **332**, 937 (2011).
 - ³⁰ E. Benckiser *et al.*, Nat. Mater. **10**, 189 (2011).
 - ³¹ A. S. Disa *et al.*, Phys. Rev. Lett. **114**, 026801 (2015).
 - ³² J. Zhang *et al.*, Nat. Phys. **13**, 864 (2017).
 - ³³ M. A. Hayward and M. J. Rosseinsky, Solid State Sciences **5**, 839 (2003).
 - ³⁴ A. Ikeda *et al.*, Applied Physics Express **9**, 061101 (2016).
 - ³⁵ Y. Gu, S. Zhu, X. Wang, J. Hu, and H. Chen, Commun. Phys. **3**, 84 (2020).
 - ³⁶ B. H. Goodge *et al.*, Proc. Natl. Acad. Sci. USA **118**, e2007683118 (2021).
 - ³⁷ Y. Fu *et al.*, arXiv:1911.03177.
 - ³⁸ D. Li *et al.*, Phys. Rev. Lett. **125**, 027001 (2020).
 - ³⁹ S. Zeng *et al.*, Phys. Rev. Lett. **125**, 147003 (2020).
 - ⁴⁰ K. W. Lee and W. E. Pickett, Phys. Rev. B **70**, 165109 (2004).
 - ⁴¹ M. F. Hundley, A. Malinowski, P. G. Pagliuso, J. L. Sarrao, and J. D. Thompson, Phys. Rev. B **70**, 035113 (2004).
 - ⁴² Y.-F. Yang, Z. Fisk, H. O. Lee, J. D. Thompson, and D. Pines, Nature **454**, 611 (2008).
 - ⁴³ J. Chen *et al.*, Sci. Rep. **9**, 12307 (2019).
 - ⁴⁴ Y. Xu, Y. Sheng, and Y.-F. Yang, arXiv:2108.03218.
 - ⁴⁵ Y. Cui *et al.*, Chin. Phys. Lett. **38**, 067401 (2021).
 - ⁴⁶ C. Lacroix, Solid State Commun. **54**, 991 (1985).
 - ⁴⁷ M. Sigrist, K. Ueda, and H. Tsunetsugu, Phys. Rev. B **46**, 175 (1992).
 - ⁴⁸ A. C. Hewson, *The Kondo Problem to Heavy Fermions*, Cambridge University Press, 1993.
 - ⁴⁹ A. Fert and P. M. Levy, Phys. Rev. Lett. **36**, 1907 (1987).
 - ⁵⁰ N. Nagaosa, J. Sinova, S. Onoda, A. H. MacDonald, and N. P. Ong, Rev. Mod. Phys. **82**, 1539 (2010).
 - ⁵¹ F. C. Zhang, C. Gros, T. M. Rice, and H. Shiba, Supercond. Sci. Technol. **1**, 36 (1988).
 - ⁵² X. Wu *et al.*, Phys. Rev. B **101**, 060504 (2020).
 - ⁵³ O. Bodensiek, R. Žitko, M. Vojta, M. Jarrell, and T. Pruschke, Phys. Rev. Lett. **110**, 146406 (2013).
 - ⁵⁴ Y. Xiang *et al.*, Chin. Phys. Lett. **38**, 047401 (2021).
 - ⁵⁵ B. Y. Wang *et al.*, Nat. Phys. **17**, 473 (2021).
 - ⁵⁶ Q. Gu *et al.*, Nat. Commun. **11**, 6027 (2020).
 - ⁵⁷ Y.-F. Yang, D. Pines, and G. Lonzarich, Proc. Natl. Acad. Sci. USA **114**, 6250 (2017).
 - ⁵⁸ M. Rossi *et al.*, arXiv:2011.00595.
 - ⁵⁹ Q. Gu and H.-H. Wen, arXiv:2109.07654.